Transactions of the Materials Research Society of Japan 30[4] 1131-1134 (2005)

Colored Carbon Hybrid Spherical Microbeads Possessing Shell Composed by TiO_2 and Iron Oxide using Cellulose-Inorganic Hybrid-sphering Technique

Kenji Arinaga,[a,c] Shoji Nagaoka,[b] Shigenori Hamaoka, [c]
Makoto Takafuji,[a] and Hirotaka Ihara[a]
[a]Department of Applied Chemistry and Biochemistry, Kumamoto University, Kumamoto 860-8555 Japan
[b]Kumamoto Industrial Research Institute, Kumamoto 862-0920 Japan
[c]Kyushu Inoac Co. Ltd., Fukuoka 812-0013 Japan
Fax: 81-96-365-5172, e-mail: nagaoka@kmt-iri.go.jp

Cellulose, which has been used in various matrix-forming materials, has long been explored as a building material. Particularly, microbeads of cellulose have been used as chromatographic packing materials, immobilization supports for microbes, and cosmetic materials. Cellulose microbeads prepared by the viscose phase-separation method, were monodispersed and spherical. We prepared the cellulose/titanium dioxide (TiO_2) and iron oxide hybrid spherical microbeads by an inorganic hybrid-sphering method based on the phase-separation phenomenon and also prepared carbon/TiO_2-anatase/Fe_2O_3 hybrid spherical microbeads by means of their carbonization for use as a photocatalyst. We also report herein the relationship between cellulose xanthate and the electronic characteristics of inorganic materials used in the inorganic hybrid-sphering process. It was found that: (1) these photoassisted-catalytic adsorbents produce a red color; (2) the reddish color of the microbeads can be controlled by changing the ratio of FeO(OH) to TiO_2; (3) the hybrid spherical microbeads are carbon spherical microbeads with a shell composed of Fe_2O_3 and TiO_2.

Key words: Cellulose, TiO_2, Iron oxide, Spherical Microbeads, Viscose Phase Separation

1. INTRODUCTION

Recent environmental applications of photocatalysis have resulted in the use of numerous photocatalysts including titanium dioxide (TiO_2), which has the ability to decompose many kinds of contaminants[1-4]. In order to achieve photodecomposition of several organic compound types, Minero et al. have examined the effects of the addition of Al_2O_3 and SiO_2 as inert supports to the TiO_2 photocatalyst suspension[5]. In addition, Taoda et al. have developed hybrid silica microbeads coated sparsely with TiO_2[6]. Nonami et al. have developed an adsorbent that partially modifies the surface of the TiO_2 particles with apatite[7]. The contact area of TiO_2 particles with organic material in the TiO_2-composite has been reduced in order to avoid the composite's photodegradation by active TiO_2 particles[8]. Using the "Phase-separation Method," we can also prepare carbon/TiO_2-anatase hybrid spherical microbeads as a photocatalyst using cellulose spherical microbeads that have been made dense with TiO_2 anatase nano-particles. In fact, the effectiveness of these microbeads in removing acetaldehyde in water as a photo-assisted catalysis has been found to be greater than naked TiO_2[9]. In the present study, we explored the possibility of hybridizing iron oxide to the above-mentioned carbon/TiO_2 hybrid spherical microbeads. Thus, we could prepare anew the photo-assisted-catalytic adsorbents with the following properties: 1) a red color, utilized as the industrial design color materials; 2) the ability to control the reddish color of the microbeads by changing the ratio of FeO(OH) to TiO_2; 3) inhibition of the photodegradation of organic components by reducing the contact area of TiO_2 with organic material containing an inorganic TiO_2 composite; and 4) the hybrid spherical microbeads are carbon spherical microbeads possessing a shell composed by Fe_2O_3 and TiO_2. We describe herein the preparation and characterization of carbon hybrid spherical microbeads covered with TiO_2 and iron oxide particles, namely colored carbon spherical microbeads.

2. EXPERIMENTAL

2.1 Cellulose/TiO_2/FeO(OH) hybrid spherical microbeads

Cellulose/TiO_2/FeO(OH) hybrid spherical microbeads were made by means of a one-step phase separation method using a cellulose xanthate aqueous solution (cellulose content, 8.9 wt%, Kojin Co. Ltd.) and a sodium polyacrylate aqueous solution (Aquaric DL-453, Mw: 50000, Nippon Shokubai Co., Ltd., Osaka, Japan). TiO_2 powder (P25, Degussa Co. Ltd., average particle size: 20 nm) and FeO(OH) powder (nacalai tesque Co. Ltd.) in the given weight ratio were slowly added to a cellulose xanthate aqueous solution (1000 g). The cellulose xanthate aqueous solution dispersing a mixture of TiO_2, and FeO(OH) particles was mixed with an aqueous solution (3500 g) containing sodium polyacrylate (340 g) and 28.6 g of $CaCO_3$ (Okutama Kogyo Co. Ltd.). These materials were then suspended by stirring at 80 °C for 30 min. After heating and congealing, the obtained hybrid spherical microbeads were washed successively with a diluted hydrochloric acid aqueous solution and water.

2.2 Carbon/TiO_2 hybrid spherical microbeads

The carbonization of cellulose/TiO_2/FeO(OH) hybrid spherical microbeads was carried out in the following four steps: (1) freeze-drying process; (2) dehydration: the hybrid spherical microbeads were dehydrated by heating at 300 °C *in vacuo* for 5 h. (CTF02); (3) carbonization: the carbonized microspheres were heated to 600 °C for over 5 h and then allowed to stand for 4 h (CTF03) under a stream of nitrogen gas; and (4) thermal treatment at 500 °C using CO_2 gas to achieve conversion of the Fe_3O_4 contained in microbeads to Fe_2O_3 (CTF04 series). As a result, particles with diameters of around 50 mm were obtained. As a reference, the Carbon/TiO_2 hybrid spherical microbeads (CT03, TiO_2 content: 40 wt%) without iron oxide were also prepared by (1), (2) and (3) procedures.

2.3 Measurement

Laser micrographs of the hybrid spherical microbeads were obtained using a laser microscope (KEYENCE VK-9500). X-ray diffraction was carried out using an X-ray Diffractometer (Rigaku RINT 2000). Electron probe micro analysis was carried out using JEOL JXA-8900 WD/ED. The colors of the beads were evaluated by specular reflectance excluded (SCE) using a Spectrophotometer CM-2002 (Konica Minolta Sensing, Inc.). The color evaluation was represented by $L^*a^*b^*$, as established by the International Commission on Illumination (CIE). Diffuse reflectance spectra were measured with a UV-VIS spectrophotometer with integrating sphere equipment (JASCO V-560 / ISV-469, JASCO, Tokyo, Japan). The zeta potentials of TiO_2 powder were measured by electrophoresis using the Laser Doppler method (Zetasizernano, Sysmex Corporation, Kobe, Japan). The catalytic evaluation was carried out by the gas-bag method. A given amount of photocatalyst powder (naked TiO_2, P25, Degussa Co. Ltd, CTF04-48: Fe_2O_3; 48 % and CTF04-94: Fe_2O_3; 5 %) which was set in a shared culture made from a polytetrafluoroethylene plate, was left in a 5 l bag packed with 40 ppm of acetaldehyde gas. The bag was then illuminated with two 20 W black lights (TOSHIBA FL20BLB: 300-400 nm). After a given time of illumination, the aldehyde concentrations were monitored using an acetaldehyde gas detector tube.

3. RESULTS AND DISCUSSION

We examined the addition of iron oxide to the sphering system by the phase separation method in order to add color. The hybridized spherical microbeads were made by a one-step phase separation method using a cellulose xanthate aqueous solution, TiO_2 particles, FeO(OH) particles, and a sodium polyacrylate aqueous solution. Figure 1(a) shows the X-ray diffraction pattern for the microbeads that were obtained by

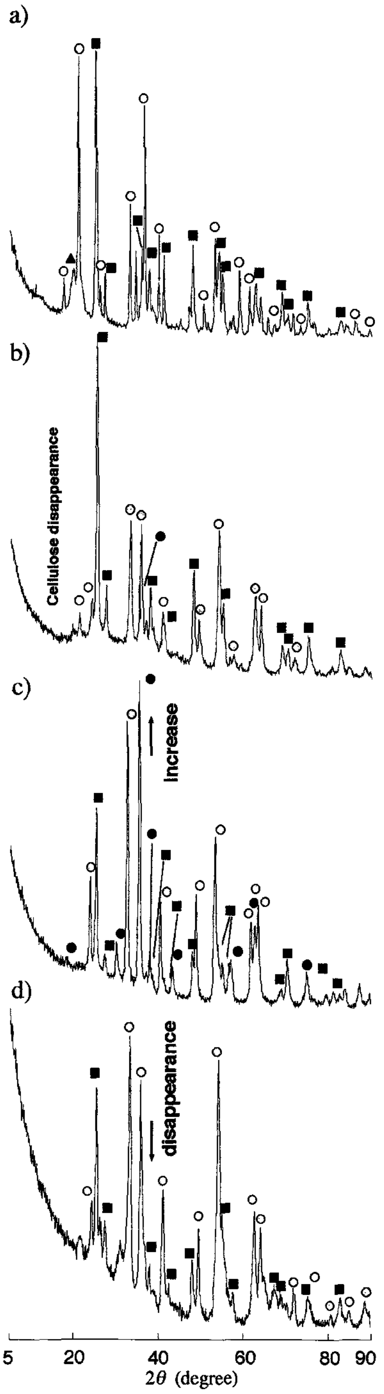

Figure 1. X-ray diffraction of hybrid spherical microbeads.
a) Cellulose/TiO_2/FeO(OH) microbeads (CTF01)
b) Dehydrated microbeads (CTF02)
c) Carbonized microbeads (CTF03)
d) Oxidized microbeads (CTF04)
○: FeO(OH) ○: Fe_2O_3 ■: TiO_2 ●: Fe_3O_4 ▲: Cellulose

sphering. The three different peaks in the X-ray diffraction pattern belong to cellulose, TiO_2 (anatase), and FeO(OH), respectively, which constitute the sphering system, i.e. the "phase separation method". The preparation of cellulose/TiO_2/FeO(OH) hybrid spherical microbeads was then carried out (CTF01). Figure 2 shows the diffuse reflectance spectra of hybrid spherical microbeads obtained in each process. The diffuse reflectance spectrum of CTF01 showed a reflectance peak of approximately 580 nm. This reflectance spectrum corresponds to the typical reflectance of yellow color. The $L^*a^*b^*$ of CTF01 determined by spectrophotometer was: L^*: 42.0; a^*: 9.92; and b^*: 34.5. The carbonization of CTF01 was performed by the above-mentioned three steps. In the dehydration process, the X-ray diffraction pattern of cellulose disappeared, as shown in Fig. 1(b). This disappearance was caused by the thermal decomposition of cellulose. Although the X-ray diffraction pattern of TiO_2 showed no change, that of FeO(OH) changed significantly. Usually, FeO(OH) is converted to Fe_2O_3 by dehydration, as shown in reaction (1). In the X-ray diffraction pattern for the product obtained by dehydration, a small peak appearing at $2\theta=35.440$ belonged to Fe_3O_4. This phenomenon indicates that FeO(OH) was partially converted to Fe_3O_4. Therefore, the product was colored black due to Fe_3O_4, which is caused by the CO gas produced by the thermal decomposition of cellulose, as shown in reaction (2).

$2FeO(OH) \rightarrow Fe_2O_3 + H_2O$ (1)

$3Fe_2O_3 + CO \rightarrow 2Fe_3O_4 + CO_2$ (2)

Figure 1(c) shows the X-ray diffraction pattern of CTF03. Although the hybrid spherical microbeads were heated in a stream of N_2 gas at 600 °C, the X-ray diffraction pattern of TiO_2 showed no change. In contrast, the X-ray diffraction pattern of Fe_2O_3 was precisely converted to that of Fe_3O_4. Therefore, the hybrid spherical microbeads obtained by the carbonizing process showed magnetic properties. The diffuse reflectance spectra of CTF02 and CTF03 showed no reflectance peak because their surfaces became black, as shown in Fig. 3. The color of Fe_3O_4 is black, as is that of amorphous carbon, i.e., L^*: 23.7, a^*: -1.10, and b^*: -0.06. The X-ray diffraction pattern of CTF04 is shown in Fig. 1(d). The X-ray diffraction pattern of Fe_3O_4 changed significantly to that of Fe_2O_3. Figure 3(a), (b) and (c) show a laser micrograph and the EPMA photo-mappings of Fe and Ti, respectively, of CTF04. The EPMA confirmed that TiO_2 and Fe_2O_3 were fixed on the surface, accounting for the beads' red color, as shown in the laser micrograph in Fig. 3(a). As shown in Fig. 2, the diffuse reflectance spectrum of CTF04 showed a broad reflectance peak from around 600 to 800 nm. This reflectance spectrum corresponds to the typical reflectance of red color. Their $L^*a^*b^*$ indicated L^*: 40.4, a^*: 13.0, and b^*: 14.9 near the value of the $L^*a^*b^*$ of naked Fe_2O_3. Figure 3(d), (e) and (f) show SEM image, the EPMA photo-mapping of Fe and Ti for the CTF04 cross section, respectively. It was confirmed that hybrid spherical microbeads were the carbon microbeads covered with TiO_2 and Fe_2O_3 and that therefore possessed a shell-structure composed of TiO_2 and Fe_2O_3. This phenomenon can be attributed to the surface electric potential of TiO_2 and FeO(OH) particles in sphering actually being homogeneously minus potentials. It can also be explained by the zeta potentials of TiO_2 and Fe(OH) particles. We have recently confirmed that the distributions of TiO_2 particles contained on hybrid spherical microbeads depend upon the composition of TiO_2

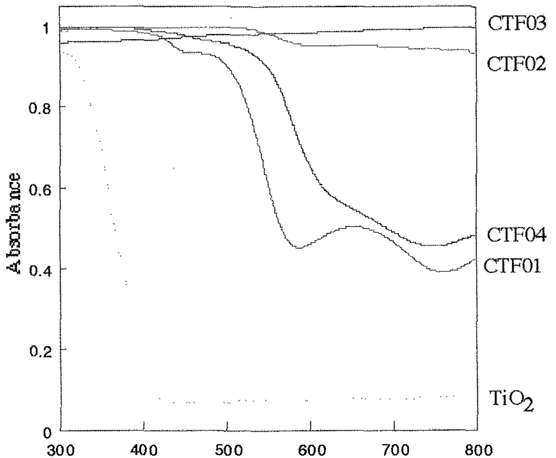

Figure 2. Diffuse reflectance spectra of CTF01, CTF02, CTF03, CTF04 and TiO_2.

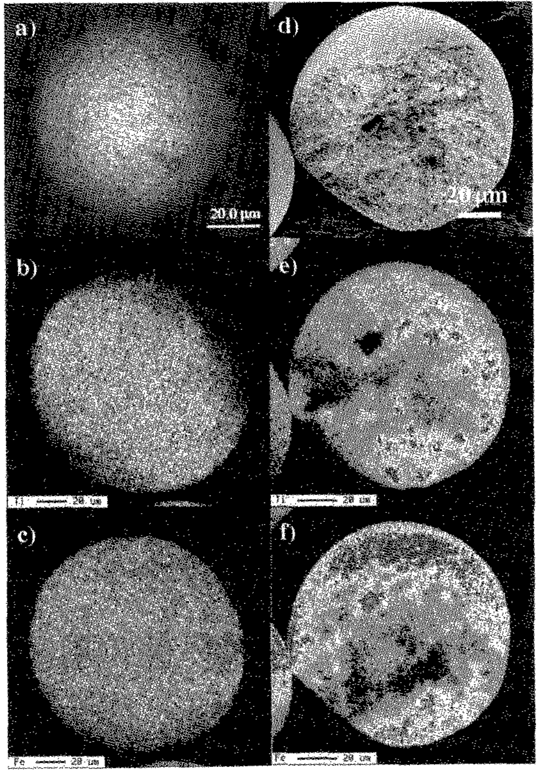

Figure 3. Laser micrograph and EPMA photo-mappings of CTF04.
(a) Laser micrograph
(b) EPMA photo-mappings for Ti on the surface,
(c) EPMA photo-mappings for Fe on the surface,
(d) SEM image of the cross section
(e) EPMA photo-mappings for Ti of the cross section
(f) EPMA photo-mappings for Fe of the cross section

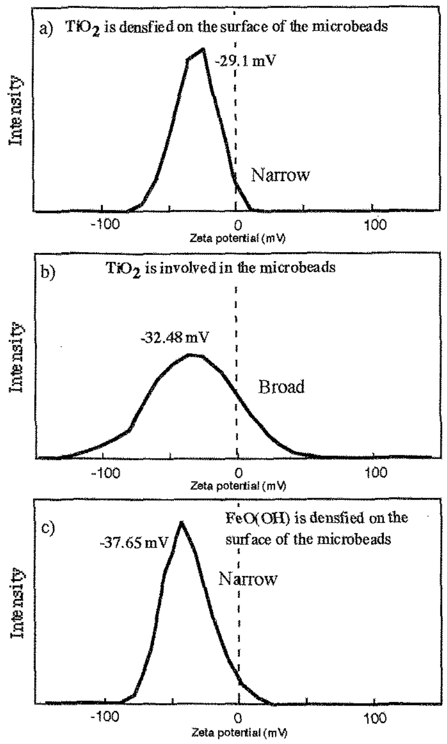

Figure 4. Zeta potential distributions of TiO_2 (P-25 (a) and ST-01 (b)) and FeO(OH) (c) measured by laser Doppler method

particles[10]. Our findings indicate that TiO_2 particles (P-25, Degussa Co. Ltd.) uniformly possessing a minus potential (as shown in Fig. 4(a)) were driven out by the following: the CSS^- group of cellulose xanthate; the COO^- group of polyacrylic acid; and the TiO_2 particles localized at the interface between the cellulose xanthate aqueous solution phase and the polyacrylic acid aqueous solution phase. As a result, we obtained cellulose/TiO_2 hybrid spherical microbeads with surfaces densely covered with TiO_2 particles. In contrast, inorganic materials (as shown in Fig. 4(b)) such as TiO_2 (ST-01, Ishihara Sangyo Kaisha, Ltd.), for which the zeta potential distributions are diffused to a plus electric potential (more than +60 mV), are located within the cellulose xanthate phase in hybrid-sphering. Therefore, the microbeads involved with TiO_2 particles were able to be prepared. On the other hand, since both the TiO_2 and FeO(OH) particles adopted in this sphering possessed a homogeneous minus potential in alkaline aqueous solution as shown in Fig. 4(a) and (c), they were driven out by the CSS^- group of cellulose xanthate and the COO^- group of polyacrylic acid, as in the case of the preparation of cellulose/TiO_2 spherical microbeads. Therefore, TiO_2 and FeO(OH) particles were localized at the interface between the cellulose xanthate phase and the PAA aqueous solution phase. As a result, the carbonized microbeads possessed a shell-structure composed of TiO_2 and Fe_2O_3. We investigated the removal efficiencies of acetaldehyde gas with CTF04-48 (Fe_2O_3 content: 48 %), CTF04-94 (Fe_2O_3 content: 5 %), and CT03 (TiO_2 content: 40%) using black light (wavelength: 300-400 nm). As shown in Fig. 5, the removal efficiency for acetaldehyde gas with CTF04 was smaller than that with naked TiO_2 and CT03 particles. The more Fe_2O_3 contained in the microbeads, the smaller the photocatalytic effect of the TiO_2 decreases.

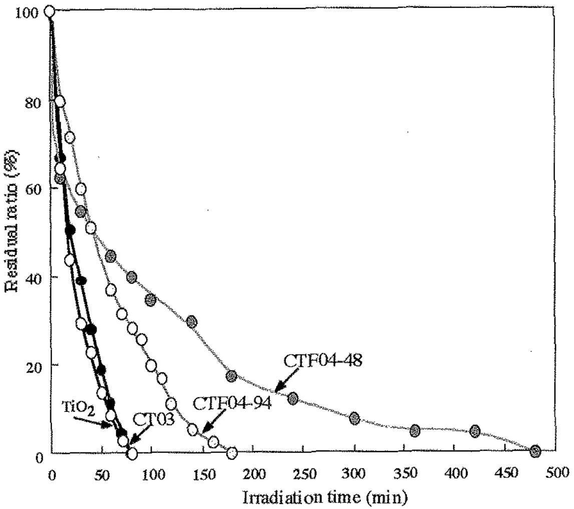

Figure 5. Removal behavior of acetaldehyde using Carbon/TiO_2/Fe_2O_3 hybrid spherical microbeads.
○: TiO_2, ●: CTF03, ○: CTF04-94, ◍: CTF04-94

In conclusion, this phenomenon can be explained by the photocatalytic effect of the TiO_2 particles being inhibited by the shielding of TiO_2 particles from photo-illumination with Fe_2O_3 particles. As such, it appears that the photo-degradation of organic components contained in TiO_2-composite materials can be inhibited due to the contact area of TiO_2 with organic components being reduced because of Fe_2O_3 particles.

REFERENCES

[1] H. Tahiri, Y. Ichou, J. Harrmann, *J. Photochem. Photobiol. A: Chem.* **114**, 219-226(1998).

[2] C.Lettmann, K. Hildenbrand, H.Kisch, W. Macyk, W. F. Maier, *Appl. Catal. B: Enviromenta,l* **32**, 215-227 (2001)

[3] Y. Zhang, J. C. Crittenden, D. W. Hand, D. L. Perram, *J. Solar Energy Engineering,* **118**, 123-129(1996).

[4] T. Torimoto, H. Yoneyama, Catal. Today, **58**, 133-140 (2000).

[5] Minero, F. Catozzo, E. Pelizzetti, *Langmuir*, **8**, 481-486 (1992).

[6] H.Taoda, M.Fukaya, E. Watanabe and K. Tanaka, *Proc. of 19th Korea-Japan International Seminar on Ceramics,* 471-475 (2002).

[7] H.Taoda, M.Fukaya, E. Watanabe and K. Tanaka, *Proc. of 19th Korea-Japan International Seminar on Ceramics,* 471-475 (2002).

[8] T. Ibusuki, K. Takeuchi, *J. Mol. Catal.* **88,** 93-102 (1994).

[9] S. Nagaoka, Y. Hamasaki, S. Ishihara, M. Nagata, K. Iio, C.Nagasawa, and H. Ihara, *J. Mol. Cat. Chem. A*, **177**, 255-263 (2002).

[10] S. Nagaoka, K. Arinaga, H. Kubo, S. Hamaoka, T. Toshsihiko, M. Takafuji, H. Ihara, *Polym. J.*, in prints.

(Received December 23, 2004; Accepted September 15, 2005)